

# Detrital garnet petrology challenges Paleoproterozoic ultrahigh-pressure metamorphism in western Greenland

Jan Schönig<sup>1</sup>, Carsten Benner<sup>1</sup>, Guido Meinhold<sup>2</sup>, Hilmar von Eynatten<sup>1</sup>, N. Keno Lünsdorf<sup>1</sup>

<sup>1</sup>Department of Sedimentology and Environmental Geology, Geoscience Centre Göttingen, University of Göttingen, Göttingen, D-37077, Germany

<sup>2</sup>Institute of Geology, TU Bergakademie Freiberg, Freiberg, D-09599, Germany

Correspondence to: Jan Schönig (jan.schoenig@uni-goettingen.de)

## Supplementary Figures

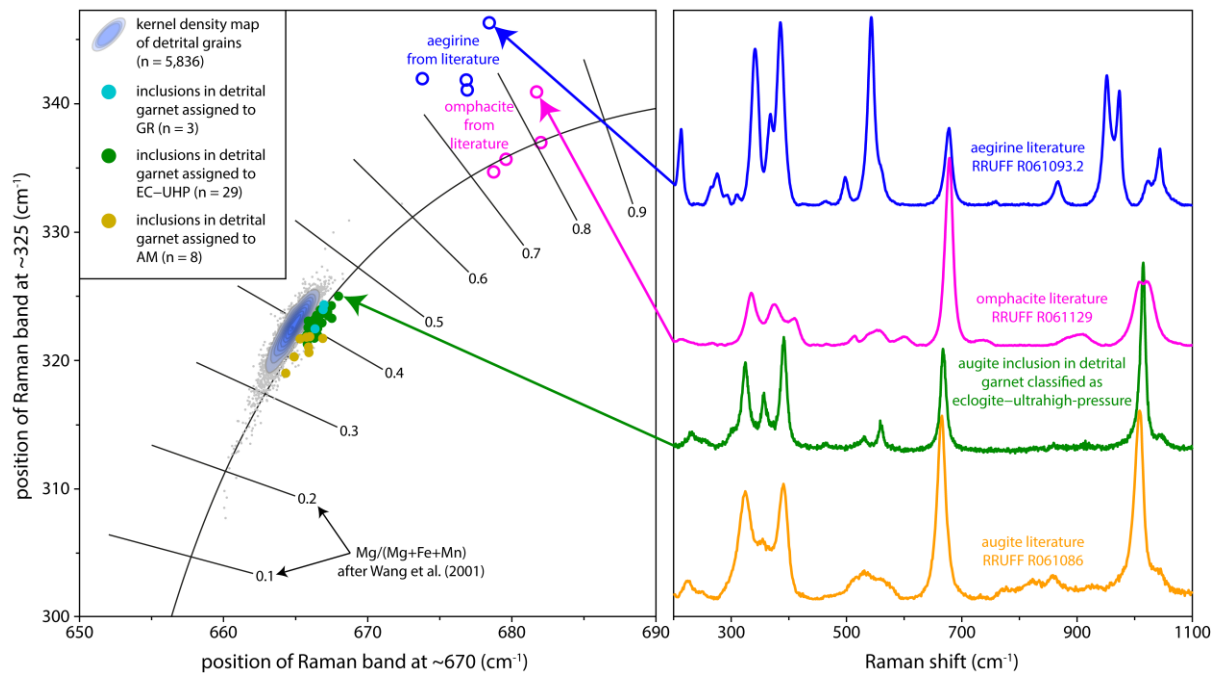


**Figure S1: Raman main band positions of clinopyroxenes.** Shown are detrital clinopyroxenes from the heavy-mineral assemblages as kernel density map as well as clinopyroxene inclusions in garnet assigned to different classes after Schönig et al. (2021b). For comparison, band positions and Raman spectra of augite, omphacite, and aegirine are shown (Zhang et al., 2005; Lafuente et al., 2015; Lin et al., 2020). Clinopyroxene composition expressed as  $Mg/(Mg+Fe+Mn)$  after Wang et al. (2001). Abbreviations: GR – granulite facies, EC-UHP – eclogite-ultrahigh-pressure facies, AM – amphibolite facies.

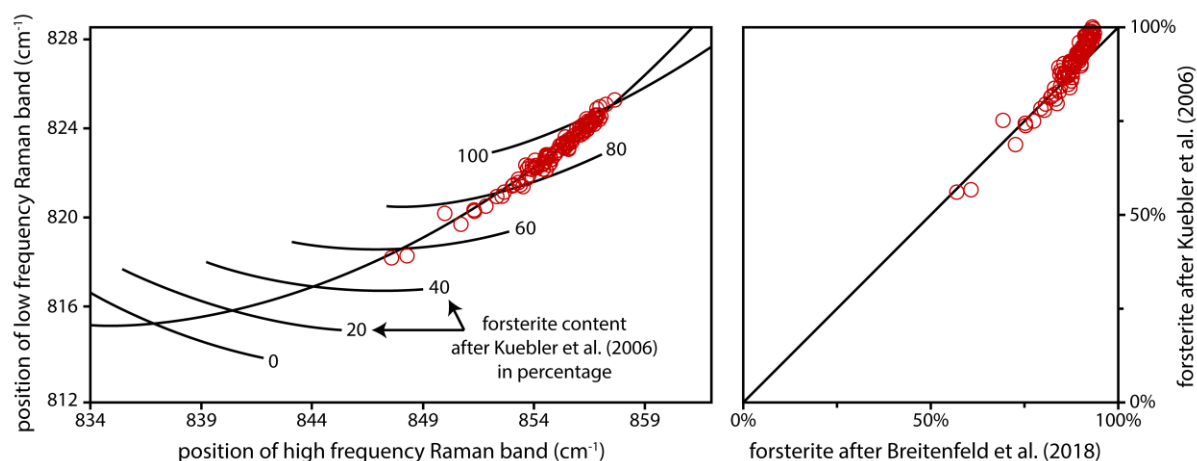


**Figure S2: Raman main band positions of olivine grains from detrital heavy-mineral assemblages ( $n = 111$ ). Left panel shows forsterite content after Kuebler et al. (2006) and right panel shows a comparison to Breitenfeld et al. (2018).**

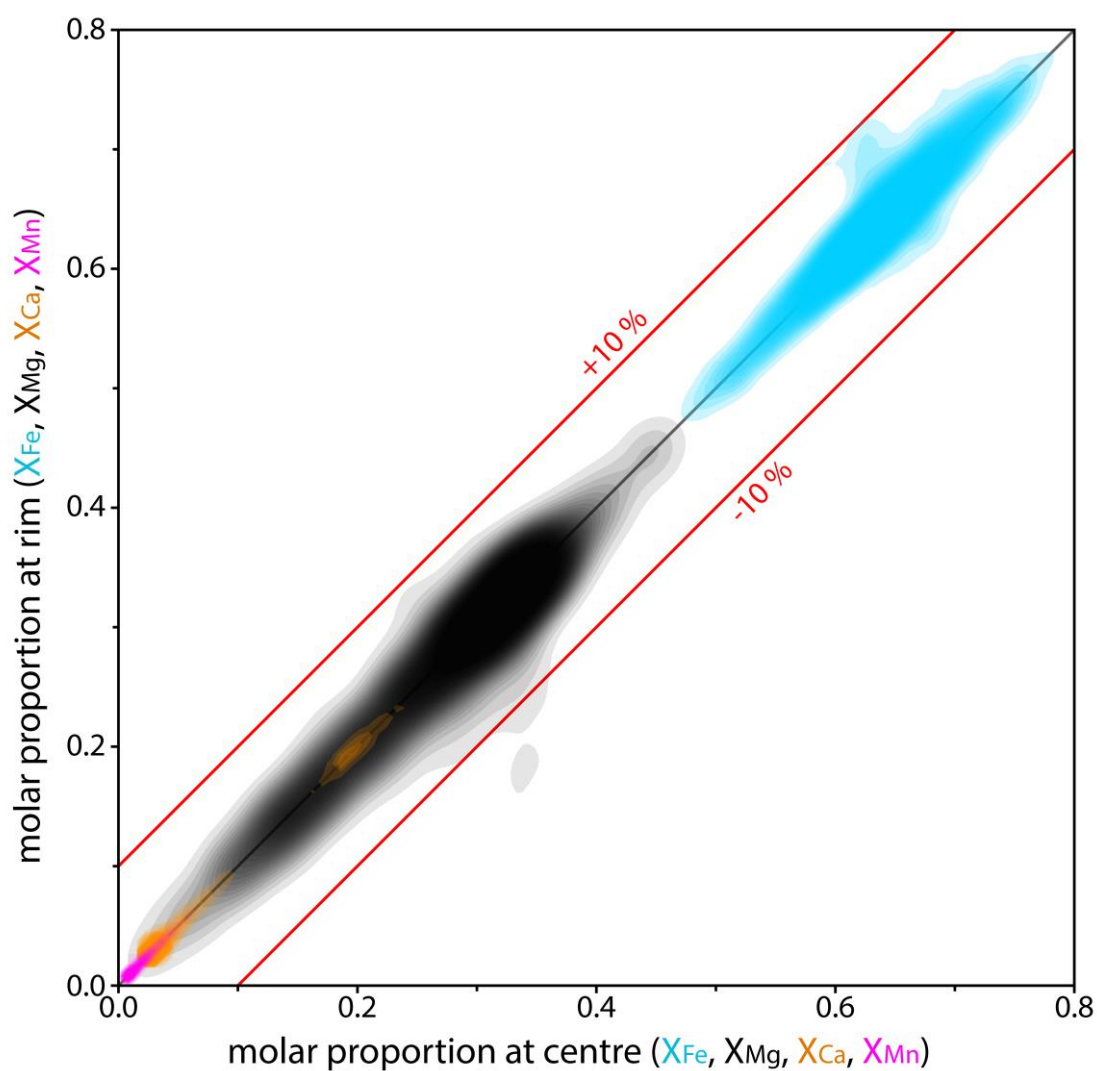


**Figure S3: Compositional variations between electron microprobe spots set at the garnet centres and those set at the garnet rims, shown as kernel density estimate maps for  $X_{Fe}$ ,  $X_{Mg}$ ,  $X_{Ca}$ , and  $X_{Mn}$  ( $n = 2,416$ ). Dataset is given in Table S2 in the Supplement.**

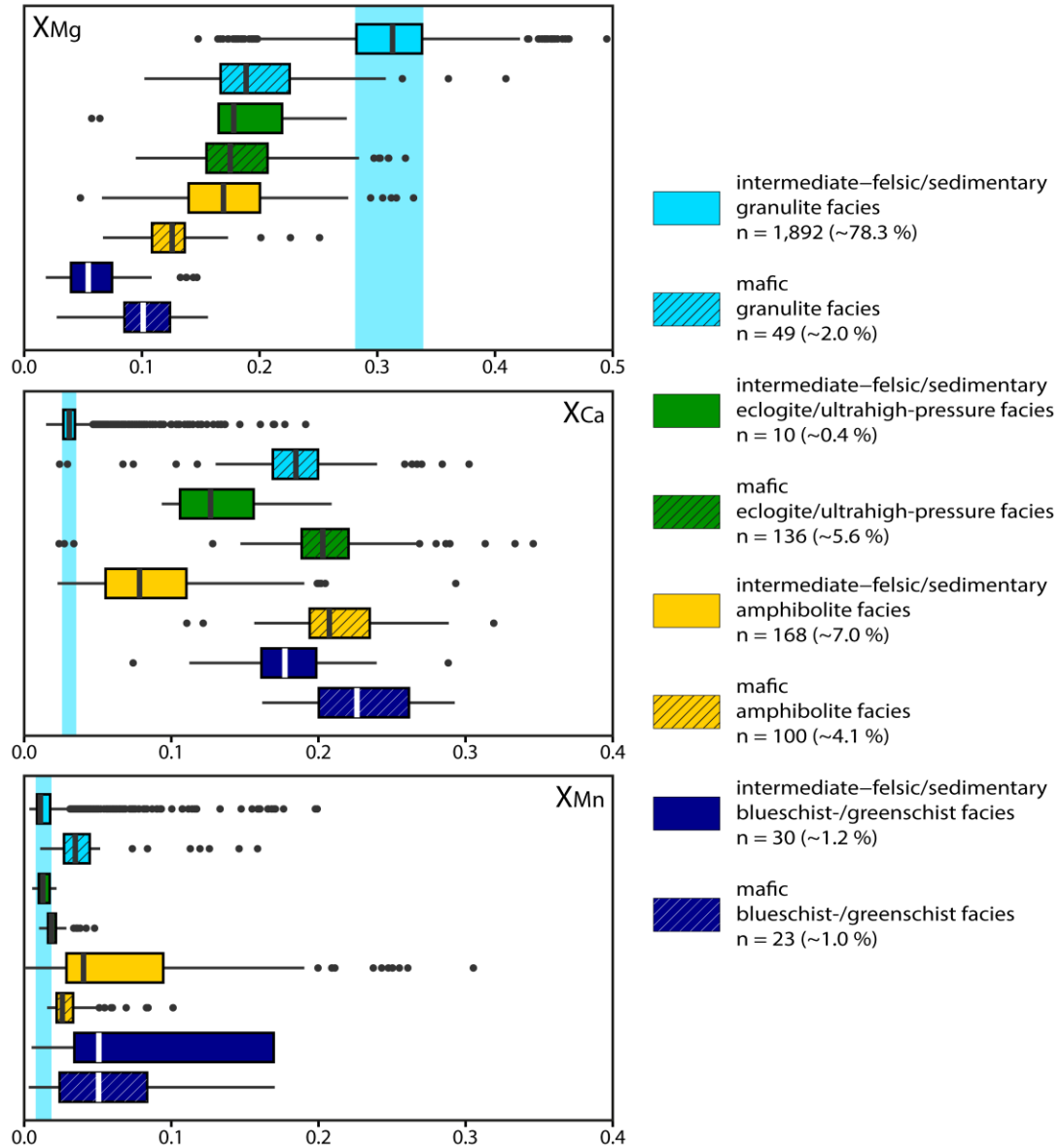


**Figure S4: Compositional difference of garnet predicted to be sourced from intermediate-felsic-sedimentary granulite-facies rocks compared the other metamorphic prediction classes. Dataset is given in Table S2 in the Supplement.**

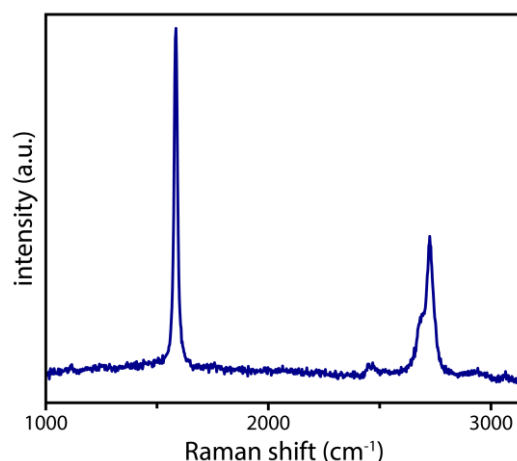


Figure S5: Example Raman spectrum of graphite inclusion in garnet number 35 from the 125–250  $\mu\text{m}$  fraction of sample JS-NGO-01s, predicted to be sourced from a blueschist–greenschist facies metamorphic rock after Schönig et al. (2021b).

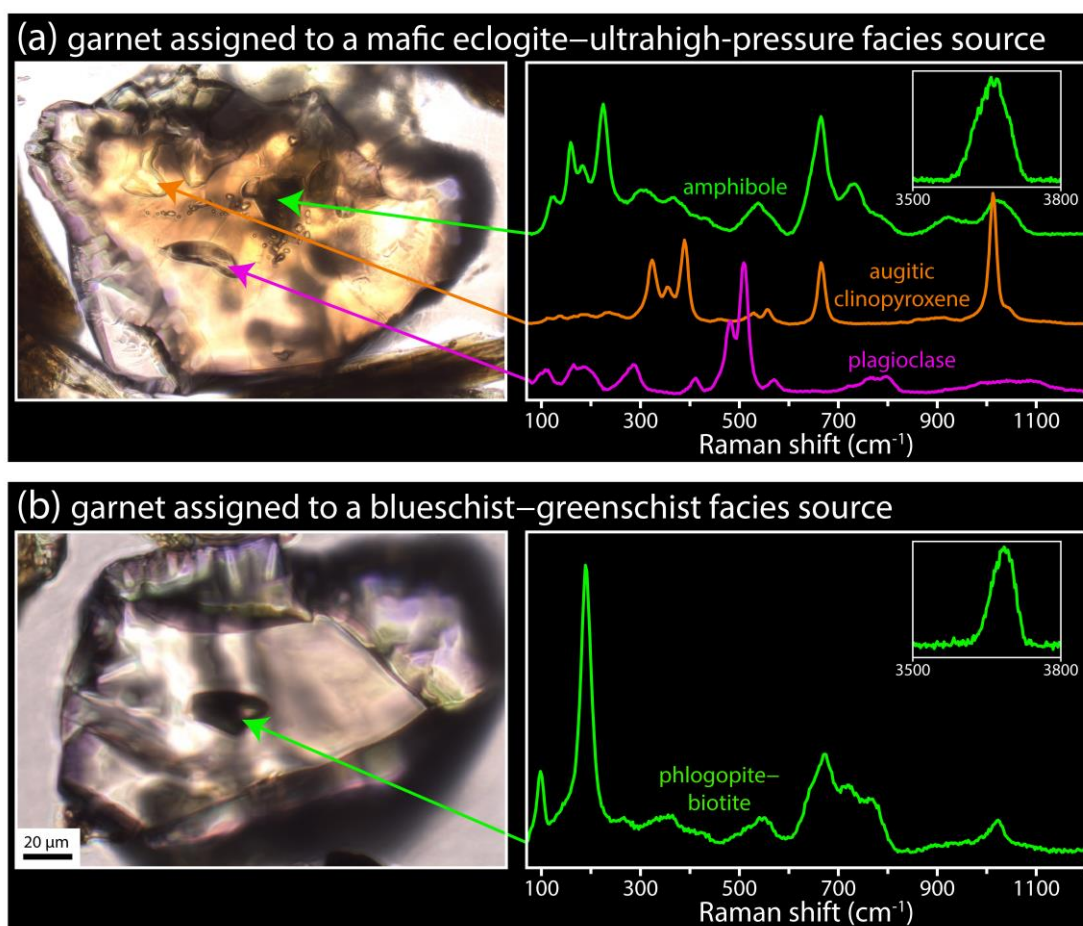
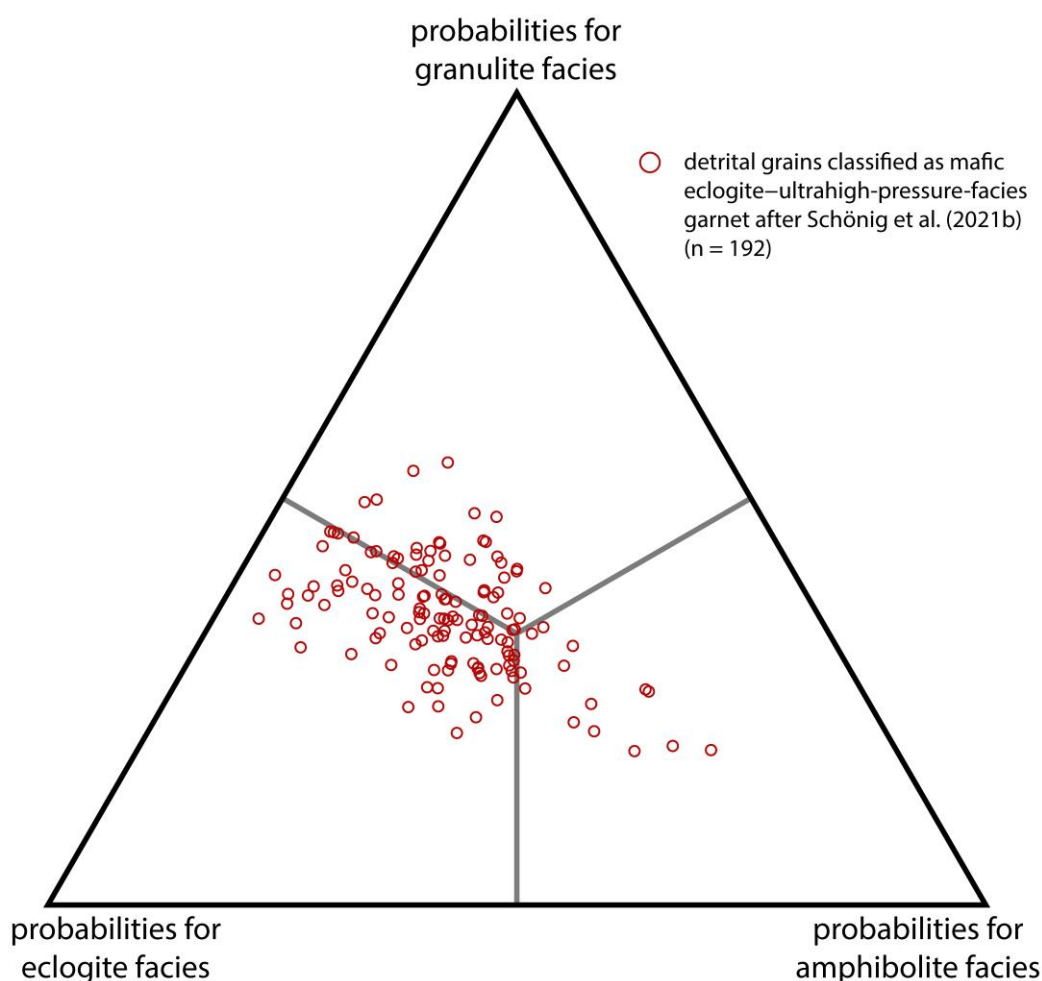


Figure S 6: Photomicrographs and Raman images showing inclusion characteristics. (a) Garnet number 7 from the 125–250  $\mu\text{m}$  fraction of JS-NGO-03s, which is predicted to be sourced from an eclogite–ultrahigh-pressure-facies rock of mafic composition based on major-element discrimination after Schönig et al. (2021b) and hosts inclusions of amphibole, augitic clinopyroxene, and plagioclase. (b) Garnet number 67 from the 63–125  $\mu\text{m}$  fraction of JS-NGO-17s, which is predicted to be sourced from a blueschist–greenschist-facies rock of mafic composition based on major-element discrimination after Schönig et al. (2021b) and hosts an inclusion phlogopite–biotite. Datasets are given in Table S2 and S3 in the Supplement.



**Figure S7: Probabilities for an amphibolite, granulite, and eclogite facies origin after Tolosana-Delgado et al. (2018) for garnets classified as being sourced from mafic eclogite-ultrahigh-pressure rocks after Schönig et al. (2021b). Prior probability 'equal-M' was used for the discrimination scheme of Tolosana-Delgado et al. (2018).**

## References

- Breitenfeld, L. B., Dyar, M. D., Carey, C. J., Tague Jr, T. J., Wang, P., Mullen, T., and Parente, M.: Predicting olivine composition using Raman spectroscopy through band shift and multivariate analyses, *Am. Mineral.*, 103, 1827–1836, doi: 10.2138/am-2018-6291, 2018.
- Kuebler, K. E., Jolliff, B. L., Wang, A., and Haskin, L. A.: Extracting olivine (Fo–Fa) compositions from Raman spectral peak positions, *Geochim. Cosmochim. Acta*, 70, 6201–6222, doi: 10.1016/j.gca.2006.07.035, 2006.
- Lafuente, B., Downs, R. T., Yang, H., Stone, N.: The power of databases: The RRUFF project, in: *Highlights in Mineralogical Crystallography*, edited by: Armbruster, T. and Danisi, R. M., De Gruyter, Berlin, 1–30, 2015.
- Lin, C., He, X., Lu, Z., and Yao, Y.: Phase composition and genesis of pyroxenic jadeite from Guatemala: insights from cathodoluminescence, *RSC Adv.*, 10, 15937–15946, doi: 10.1039/D0RA01772H, 2020.
- Schönig, J., von Eynatten, H., Tolosana-Delgado, R., and Meinhold, G.: Garnet major-element composition as an indicator of host-rock type: a machine learning approach using the random forest classifier, *Contrib. Mineral. Petrol.*, 176, 98, doi: 10.1007/s00410-021-01854-w, 2021b.
- Tolosana-Delgado, R., von Eynatten, H., Krippner, A., and Meinhold, G.: A multivariate discrimination scheme of detrital garnet chemistry for use in sedimentary provenance analysis, *Sed. Geol.*, 375, 14–26, doi: 10.1016/j.sedgeo.2017.11.003, 2018.

Wang, A., Jolliff, B. L., Haskin, L. A., Kuebler, K. E., and Viskupic, K. M.: Characterization and comparison of structural and compositional features of planetary quadrilateral pyroxenes by Raman spectroscopy, *Am. Mineral.*, 86, 790–806, doi: 10.2138/am-2001-0703, 2001.

Zhang, L., Song, S., Liou, J. G., Ai, Y., and Li, X.: Relict coesite exsolution in omphacite from Western Tianshan eclogites, China, *Am. Mineral.*, 90, 181–186, doi: 10.2138/am.2005.1587, 2005.